0013-7227/00/$03.00/0
Endocrinology

Vol. 141, No. 11
Printed in U.S.A.

Estrogen Deficiency, Obesity, and Skeletal Abnormalities in Follicle-Stimulating Hormone Receptor Knockout (FORKO) Female Mice*

NATALIA DANILOVICH†, P. SURESH BABU, WEIRONG XING†, MARIA GERDES, HANUMANTHAPPA KRISHNAMURTHY, AND M. RAM SAIRAM

Molecular Reproduction Research Laboratory, Clinical Research Institute of Montréal, Montréal, Québec H2W 1R7, Canada

ABSTRACT

Targeted disruption of the receptor for glycoprotein hormone, FSH (FSH-R) causes a gene dose-related endocrine and gametogenic abnormality in female mice. The resulting FSH-R knockout (FORKO) mutants have disordered estrous cycles, ovulatory defects, and atrophic uterus. The heterozygous animals that initially show reduced fertility undergo early reproductive senescence and stop breeding altogether. Lack of FSH-R signaling in females causes severe ovarian underdevelopment producing chronic estrogen deficiency. This was accompanied by increases in serum testosterone levels. Ovarian aromatase gene transcription and translation are unaltered in the mutants. Early loss of estrogen in the null mutants leads to obesity and skeletal abnormalities that intensify with age producing (kyphosis), a hunchback appearance. Both these changes also become apparent in older heterozygous mice coincident with early reproductive senescence. The expression of nuclear estrogen receptor(s) α and β genes and the corresponding proteins in the ovary and uterus of FORKO mice appear to be intact. The loss of ovarian estrogen creates an imbalance in A and B forms of the progesterone receptor in the uterus of both heterozygotes and null mutants. Some of the changes we have documented here in FORKO mice are reminiscent of the ovarian dysfunction and other major symptoms that are usually associated with estrogen deficiency. In null mutants, estradiol-17β administration promptly induced uterine growth and reversed the accumulation of adipose tissue indicating that estrogen receptors are functional. Thus, the phenotypes evident in these genetically altered FSH-R mutants may provide an experimental system to explore the effects of estrogenic compounds on different targets including the ovary in a nonsurgical setting. (*Endocrinology* **141:** 4295–4308, 2000)

AMONG THE TROPHIC regulators of gonadal function are three members of the glycoprotein hormone family namely FSH, lutropin of the pituitary, and CG of the placenta in human and equidae (1, 2). The latter two being structurally and functionally homologous, signal through the same G protein-coupled receptor (3), whereas FSH functions by binding to its own receptor(s) in ovarian and testicular cells (4). The cloning and expression of FSH-Rs with different receptor motifs (5, 6) arising from the alternative splicing of the single large gene (7, 8) has suggested multiple pathways of signaling including Gs coupled and growth factor types of action (9). These are also consistent with crystallographic evidence suggesting growth factor motifs for signaling in the glycoprotein hormones (10).

Although there is extensive structural and functional similarities among the oligomeric glycoprotein hormones that also includes pituitary TSH, each ligand is highly selective in it's binding to specific receptor(s) in target cells. In the female, the FSH-R is expressed exclusively in the granulosa cells of the developing ovary where it coordinates the growth of the follicle to support ovum maturation (11). The FSH-Rs in follicles destined to become dominant and ovulate come under the influence of neuroendocrine mechanisms via the secretion of pituitary FSH.

The important role of pituitary FSH signaling in ovarian development and function has been reinforced by recent genetic studies in humans as well as experimental animals. Finnish women homozygous for a point mutation, which alters a single amino acid Ala 189 to Val, are infertile due to primary amenorrhea. This mutation in the 7th exon of extracellular domain of the receptor leads to a large reduction in FSH-R signaling compromising ovarian development (12, 13). Men with the same mutation also show deficient testicular function and infertility to varying degree (14). A different receptor mutation of the activating type (D567G) in the third intracytoplasmic loop supports spermatogenesis and fertility in a man without the need for the pituitary hormone, FSH (15). Some genetic mutations of the hormone FSH-β subunit leading to premature terminations in the mRNA produce a nonfunctional hormone causing infertility in the affected individuals (16–18). Similarly, female mice where one of the exons of the FSH-β subunit has been disrupted by homologous recombination are also infertile because of failure of ovarian development beyond a critical stage (19).

The critical role of FSH receptor signaling for gonadal function to ensure species propagation emphasizes why mutations in the ligand and receptor are not common. To understand in more detail the physiological role of FSH-R signaling, we recently generated mutant mice in which all forms including the alternatively spliced variants of the receptor

Received May 1, 2000.
Address all correspondence and requests for reprints to: M. Ram Sairam, Ph.D., Molecular Reproduction Research Laboratory, Clinical Research Institute of Montréal, 110 Pine Avenue West, Montréal (Québec), H2W 1R7, Canada. E-mail: sairamm@ircm.qc.ca.
* This investigation was supported in part by the Canadian Institutes of Health Research.
† Holders of doctoral research awards from the Canadian Institutes of Health Research.

have been eliminated (4). Mutant females exhibit profound changes in ovarian structure and secondary sex organs that remain infantile. Lack of ovulation causes sterility in the mutants. The overall phenotype mimics hypergonadotropic-hypogonadism seen in infertile women. Further analysis of these mutant females was prompted by the severe atrophy of the uterus as well as important visible external changes that developed upon aging. Evidence presented here reveals that FSH-R gene disruption causes complete loss of estrogen production from the ovary. As one of the important steroid hormones in the body, estrogen has genomic as well as non-genomic effects (20). Its genomic actions are exerted via nuclear receptors of which two (ER-α,β) are presently well characterized (21, 22). Our work demonstrates that lack of estrogen due to the loss of FSH-R signaling in mice also causes important metabolic alterations that induce obesity and skeletal abnormalities. These disturbances are similar to changes that occur in postmenopausal women whose ovaries cease to function following the cessation of reproductive life and natural loss of FSH-R's despite the presence of high hormone (FSH) levels in circulation. Because heterozygous female mice also undergo early senescence and exhibit the above abnormalities around this time, these mutants may be useful in exploring the physiological and molecular changes associated with loss of estrogen's actions. As part of the phenotypic characterization of the null mutants, we show that some of the effects consequent to the loss of FSH-R are fully reversed by treatment with estradiol-17β. Henceforth, we will refer to the FSH-R null mutants as FORKO (follitropin receptor knock out) mice. Portions of these data have been presented in preliminary form (23, 24).

Materials and Methods

Generation of FSH-R knockout mice

The generation of mice with targeted disruption of the FSH receptor has been recently described (4). The disruption strategy to delete 648 bp that also includes the coding region from the translation initiation site to the end of exon 1 assured us the elimination of all alternatively spliced forms of this receptor that normally arise from a single large gene. We have confirmed this by examining expression of the protein corresponding to the full length as well as one other alternatively spliced FSH-R that is also expressed in the normal ovary (9). Both proteins are absent in the null mutants (9, and Babu, S., N. Danilovich, and M. R. Sairam, data not shown). Breeding of the F2 generation male and female heterozygotes with the sv129 background produced animals of the three genotypes. Adult females were housed in littermate groups (five animals per cage) under standard and approved laboratory conditions with controlled illumination (12-h light, 12-h dark) and temperature (22 C) and had unrestricted access to food and water. For all experiments in this study virgin 3- to 4-month-old female mice were used with exceptions for specific examples as mentioned in the text and legends. Mice were genotyped by PCR of DNA extracted from tailpieces obtained at weaning. We designed the following set of specific primers that would unambiguously identify all three genotypes in a single multiplex PCR test. The forward and reverse primers for the FSH-R (−482 to +152) were CATGTCAGTAGTACATTAGAG and AGTTCAATGGCGTTCCG. For the Neo+ gene (sequence 415–762) AAGGGACTGGCTGCTATTG was used as forward primer with AGAAAAGCGGCCATTTTC as the reverse primer. After an initial denaturation at 94 C for 5 min, 30 cycles of PCR was performed under the following conditions. 94 C for 45 sec, annealing for 45 sec at 54 C, extension at 72 C with a final step of 10 min. Analysis on a 1% agarose gel identified the 634 bp for wild-type and the 348 bp (Neo gene) mutant fragments. Both fragments were seen in the heterozygotes (data not shown).

Estrous cycle

Three groups of adult (3–3.5 months of age) virgin female mice were used: homozygous mutants (n = 15), heterozygous (n = 15), and wild-type mice (n = 10). After one week of adaptation, the mice were examined for vaginal patency, and smears were taken daily by lavage for at least five cycles to establish the length of the estrous cycle. The estrous cycles pattern was assessed by daily examination of cellular composition of vaginal washings.

Collection of blood and adipose tissue

Heterozygous and wild-type mice were anesthetized on the morning of proestrus, as determined by the appearance of the vaginal smears. Because FORKO females were acyclic, they were used randomly on a selected day between 1000 h and 1200 h. For measurement of plasma steroid hormone levels, blood samples were collected by cardiac puncture into plastic centrifuge tubes containing EDTA. After centrifugation for 15 min at 2,500 × g, the plasma was stored at −20 C until used. Abdominal, inguinal, and retroperitoneal fat was dissected and weighed.

Histological assessment of uteri, ovaries, and vaginae

After exsanguination, the tissues (ovaries, uterus, and vagina) were removed and cleaned of fat and mesentery, blotted on filter paper, and weighed to the nearest 0.1 mg. These tissues were then fixed in 10% buffered formalin for 24 h, and processed in a tissue processor for paraffin embedding. The 5-μm sections were cut and stained by standard protocols with hematoxylin and eosin. Histological examination of the tissues was performed by light microscopy.

Assessment of skeletal abnormalities in FORKO female mice

To record skeletal changes, 4-month-old female mice under anesthesia were x-rayed in the animal facility. After taking the x-ray, some animals were killed and the weight of the right femur was taken. The femur was placed in 10% formalin for 24 h and then in 2 N HCl for decalcification. The bones were dehydrated in gradient of alcohol followed by xylene and then embedded in paraffin. Longitudinal sections of 5 μm were cut and stained using hematoxylin and eosin protocol. Bone marrow cells were prepared from the right and left tibiae as described previously by Masuzawa *et al.* (25) by flushing out the bone marrow with Ca^{2+}- and Mg^{2+}-free PBS using a syringe with a 27-gauge needle. The cells were centrifuged and resuspended in 2 ml of ammonium chloride-Tris buffer to lyse red blood cells. The cell suspension was washed with PBS three times, and resuspended in 1 ml of PBS containing 1% BSA. The cells (1×10^6) were then incubated for 30 min on ice with FITC-conjugated B220 (RA3–6B2; PharMingen), washed twice, and resuspended in free PBS containing 1% BSA. Stained cells were analyzed on a Coulter flow cytometer. Unstained cells were used as controls.

RT-PCR and Western blotting

RNA from ovary and uterus was extracted using Ambion, Inc. (USA) Midi RNA isolation and 5 μg was reverse transcribed under standard conditions in a 20 μl reaction using MMLV reverse transcriptase. Ten percent of this mixture was used in each amplification reaction. Forward and reverse primers for ERα and ERβ mRNA based on GenBank sequences (Accession Numbers M38561 and U81451, respectively) were designed using the primer optimization program available in-house. For amplifying ERα (411 bp sequence 1436–1847) the oligonucleotides AGGAATCAAGGTAAATGTGTGGAAGGC and GGCGGTGGGCATCCAACA were used as forward and reverse primers, respectively. The forward and reverse primers used for amplifying ERβ (203 bp, sequence 1018–1221) were TGGCGACGACGGCACGGT and GCTGCTGGGAAGAGATTCCACTCTT. Using the buffer B of the optimization kit from Invitrogen (San Diego, CA) facilitated these amplifications producing the predicted fragment from tissues of the wild-type that were first used as positive controls. The aromatase gene was amplified to verify production of a 504 bp (sequence 290–794) fragment using the following primers based on the mouse cDNA sequence (GenBank accession num-

ber D00659)-GAGAGTTCATGAGAGTCTGG (forward) and CCTTGACGGATCGTTCATAC (reverse). These PCR amplifications were performed at 95 C-5 min followed by 30 cycles at 94 C-40 sec, 55 C-30 sec, and 72 C-40 sec. Final extension was for 7 min. All reaction products were separated on a 1.5% agarose gel and stained with ethidium bromide. Specificity of the amplification was checked by appropriate restriction enzyme digestion. Each test sample was also simultaneously verified for amplification of cyclophilin as an internal control under identical conditions using primers CTGCAGACATGGTCAACCCCA (forward) and TTAGAGTTGTCCACAGTCGGA (reverse) generating a 500-bp fragment (sequence −8 to +492).

Western blotting of desired proteins from individual sample or pools (in case of null mutants) was performed on the same day. Fresh or frozen tissues were extracted with lysis buffer containing detergent and protease inhibitor cocktail (50 mM Tris-HCl, pH 7.2, 1% NP-40, 50 mM glycerophosphate, 5 mM DTT, 1 mM sodium vanadate, 0.05 mM NaF, 0.1 mM phenylmethylsulfonyl fluoride, and 5 μg/ml leupeptin). Fifty micrograms of protein was run on SDS-PAGE gels, transferred to nitrocellulose, for reaction with the following antibodies at a dilution of 1:500. For aromatase, the antihuman aromatase IgG supplied by Dr. E. Simpson (University of Texas, Dallas, TX) was used. ERα monoclonal antibody was obtained from Drs. G. L. Greene (University of Chicago, Chicago, IL) (MAb H222) and P. Chambon [Institut de Génétique et de Biologie Moléculaire et Cellulaire (IGBMC), Illkirch, France] (MAb B10). For PR detection, we used the Mab JZB39 from Dr. Greene. The use of these four antibodies from established investigators for detecting respective antigens is well known. For testing ERβ protein, we had access to affinity purified antipeptide ERβ IgG (sample no. 29) supplied by Dr. P. T. K. Saunders, Medical Research Council (Edinburgh, UK). This antiserum against peptide CEARSKEHTLPVNRETLKRK in the N-terminal A/B domain of hER β that is conserved across many species has been used for localizing ER β in the ovary (Saunders, P., personal communication). After treatment of the blots with 1:2000 dilution of corresponding second antibody (Santa Cruz, CA), bands were finally detected by the Amersham Pharmacia Biotech-ECL kit and compared with the reported values for molecular weight. Where necessary, an approximation of the immunoreactivity in the samples was obtained by densitometric measurements of the corresponding bands in the three genotypes.

Measurement of ovarian steroids by RIA

The estradiol-17β, progesterone, and testosterone RIAs of serum samples were performed using Coat-A-Count kits (Diagnostic Products Corp., Los Angeles, CA) with sensitivity of 1.4 pg/ml, 0.02 ng/ml, and 4 ng/dl, respectively. All RIAs were performed according to the manufacturer's instructions.

Immunohistochemistry

The sections of uteri were first deparaffinized and then treated with 3% H_2O_2 in methanol for 10 min. The sections were incubated overnight at 4 C with lactoferrin antibody (91807 ML Fab, gift from Dr. C. Teng, NIEHS, NC) at the suggested dilution of 1:500. Thin sections were processed for immunostaining using Histostain kit (Zymed Laboratories, Inc., South San Francisco, CA). Sections were washed in 0.005% Triton X-100 in PBS (pH 7.4) followed by incubation with the secondary biotinylated antibody for 10 min at room temperature. After a 5-min wash, the sections were treated with peroxidase-conjugated antibodies for 10 min. After washing in PBS, liquid diaminobenzidine was applied followed by a 10-min wash in PBS and then counterstained with hematoxylin. The intensity of immunostaining was semiquantitatively designated as weak, medium, strong or none.

Steroid hormone replacement therapy in FORKO mice

The potential effect of estrogen replacement in 4- to 5-month-old FORKO females was studied by treating them with estradiol-17β for a short duration. In experiments designed to examine uterine responses, the mice were given two sc injection of the hormone (1 μg) for 2 days and killed at 48 h. In a second experiment, the mice were treated once daily (1 μg) for 14 days to verify effects on adipose tissue. In both series, mutants treated with olive oil served as control. At the end of treatment, appropriate tissues were weighed and stored for subsequent analysis.

Statistical analysis

All data were expressed as mean ± SEM and were analyzed by one-way ANOVA. A value of $P < 0.05$ was considered to be statistically significant.

Results

Reproductive performance of the F2 generation heterozygous mice (Table 1)

Crosses of the heterozygous mice resulted in the live birth of offspring according to the traditional Mendelian distribution of genotypes. More careful scrutiny of the breeding performances over 2 years revealed additional interesting patterns. Not only did the heterozygous females conceive later (at 10–12 weeks *vs.* 7–8 weeks for wild-type), but their overall reproductive capacity was also compromised. This disturbance occurred in two ways. The heterozygous females exhibited increased interval between mating and conception that progressively got longer with each pregnancy. After about 6–8 births, the heterozygous females could no longer conceive, whereas their wild-type counterparts continued to breed for more than 14 months, producing fertile young. Another indication of suppressed reproductive potential in heterozygous females is the smaller size of litters. The loss of only one FSH-R allele was sufficient to induce more than 50% reduction in litter sizes. To eliminate any perturbation due to the use of heterozygous males, we compared breeding performance of heterozygous females mated with wild-type males. Here also, the time lag between mating and

TABLE 2. Examination of vaginal cytology

Genotype	Length of estrous cycle (days)	Duration of estrus (days)	Presence of epithelial and cornified cells
FORKO	None	None	Occasional
Heterozygous	6.6 ± 3.5[a]	1.5 ± 0.2	Normal
Wild-type	4.4 ± 0.3	2.2 ± 0.4	Normal

Values are expressed as mean SEM. [a], $P < 0.05$.

TABLE 1. Breeding performance

Number of animals	Male × Female	Period between mating and first litter (days)	Number of pups in first litter	Weaning success in first litter (%)
7 × 7	+/+ × +/+	21.4 ± 0.2	9.8 ± 0.5	95.9 ± 0.7
10 × 10	+/+ × +/−	32 ± 2.5[a]	5.6 ± 0.9[a]	75 ± 1.5[a]
16 × 16	+/− × +/−	38.2 ± 3.3[a]	4.7 ± 2.3[a]	68.7 ± 2.5[a]

Weaning success = animals surviving on day 21. All results are expressed as mean SEM.
[a], $P < 0.05$.

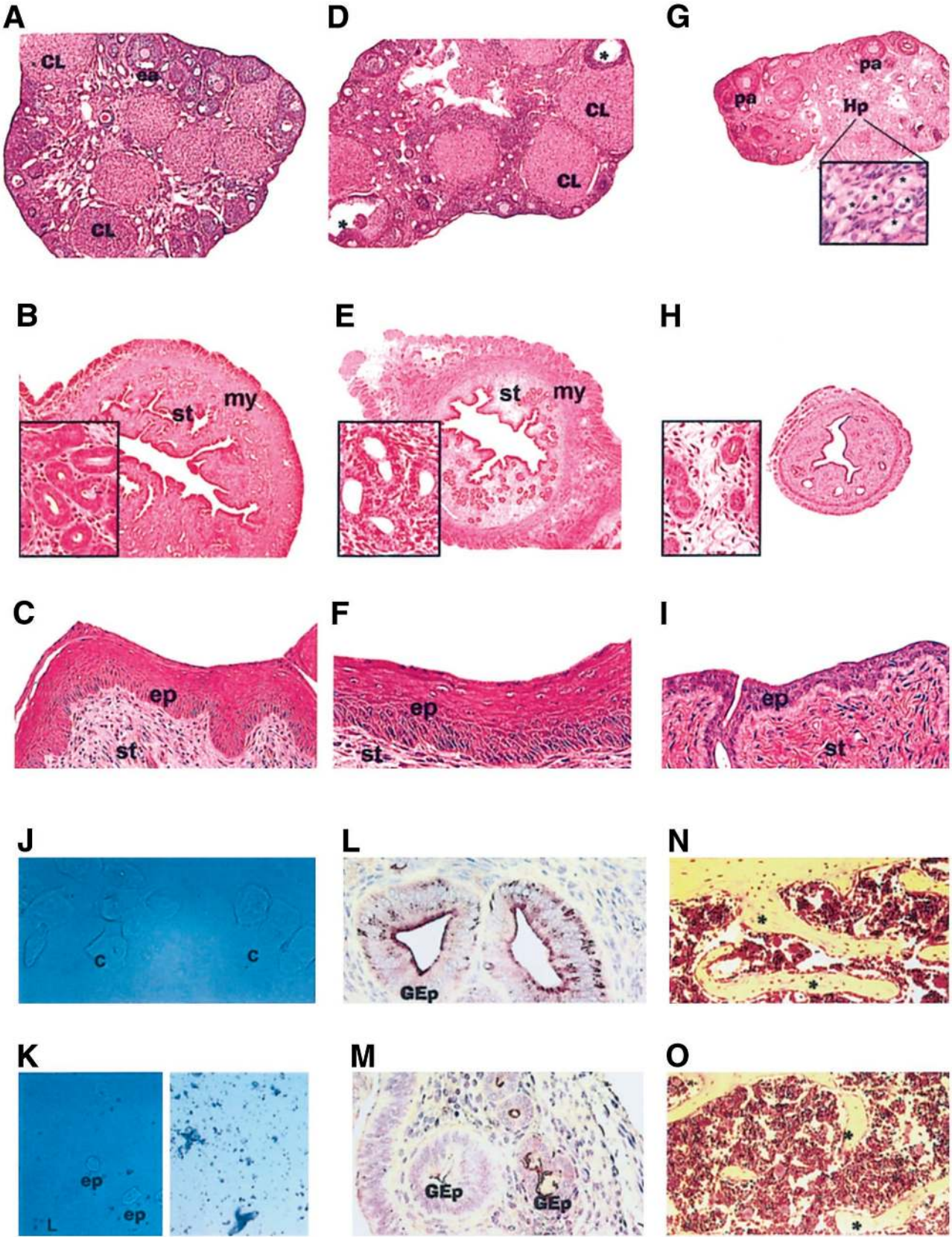

FIG. 1. Histological appearance of adult FORKO, heterozygous, and wild-type mice. Reproductive tract: A–I. Shown are sections from wild-type (A–C), heterozygous (D–F), and FORKO (G–I) female mice. Ovarian cross-sections (A, D, and G) are at low magnification (12.5×). Note the presence of preantral (pa) and early antral (ea) follicles as well as corpora lutea (CL) in both wild-type (A) and heterozygous ovary (D). In addition,

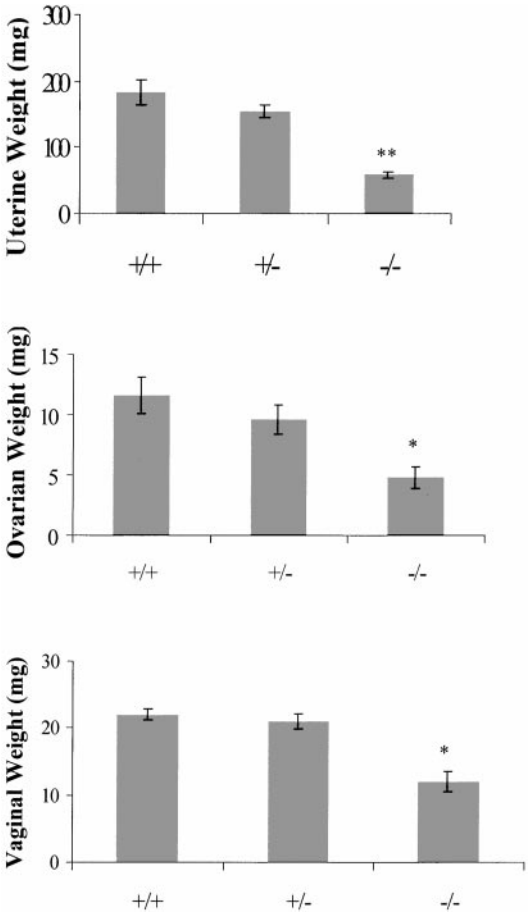

FIG. 2. Growth status of reproductive tissues in wild-type, heterozygous, and FORKO female mice. The wet weight of two ovaries, uterus, and vagina (mg) in +/+ (wild-type), +/− (heterozygous), and −/− (FORKO) are shown. Values represent the mean ± SEM for 10 animals per genotype. Comparisons were made against wild-type animals. *, $P < 0.007$, **, $P < 0.001$.

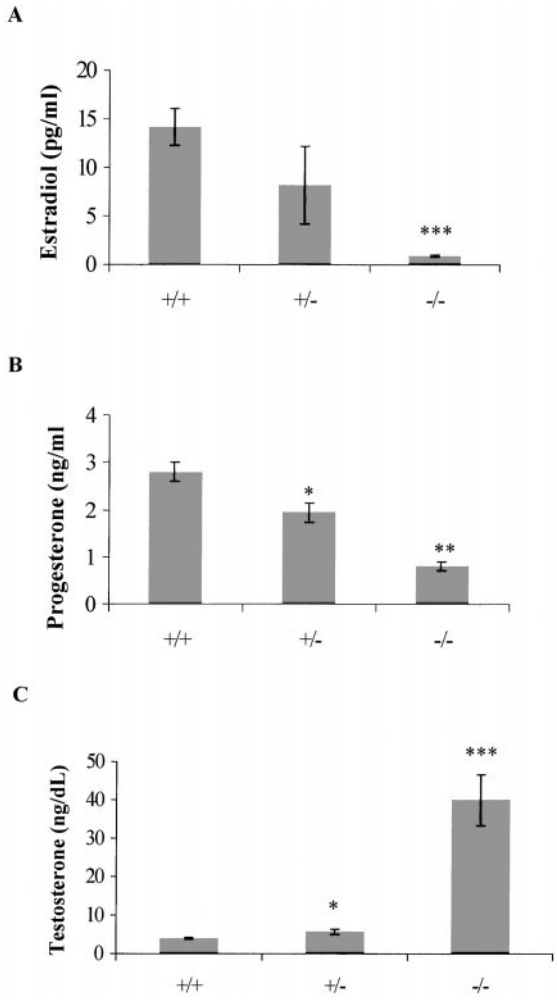

FIG. 3. Steroid hormone levels in serum of wild-type, heterozygous, and FORKO female mice. The levels of estradiol-17β (pg/ml) (A), progesterone (ng/ml) (B), and total testosterone (ng/dl) (C) of individual serum samples of +/+ (wild-type), +/− (heterozygous), and −/− (FORKO) mice determined by respective RIAs are shown. Values represent the mean ± SEM for 7–10 animals per genotype. Comparisons were made against wild-type animals. *, $P < 0.05$, **, $P < 0.005$, ***, $P < 0.002$.

first litter was significantly longer compared with the wild-type littermates, and the number of pups was also reduced by 43%. When we analyzed their success at first weaning (pups surviving on day 21), there was a significant decrease by 25% in the crosses between heterozygous female and wild-type male mice. In crosses among heterozygous breeders, the decrease was even more profound. These data clearly suggest a gene dosage effect that may lead to early reproductive senescence.

atretic follicles were noticed in heterozygous ovary (*asterisk*) (D). The FORKO ovary is characterized by the presence of few preantral follicles (pa), hyperplasia of interstitial tissue (Hp), and a lack of corpora lutea (G). The *inset* in panel G shows a higher magnification (500×) of the ovarian stroma that has hypertrophied in the FORKO ovary. *, Hyperplastic cells and features characteristic of steroid hypersecretion are evident here. Cross-sections of uterine tissue from wild-type (B), heterozygous (E), and FORKO (H) adult females show the presence of all three anatomical tissue compartments in the uteri of the wild-type and FORKO mice (12.5×). The wild-type uterine section illustrates a normal myometrium (my), endometrial stroma (st), and epithelium (ep) (B). The FORKO uterine section displays reduced diameter due to the atrophy of each compartment (H). The heterozygous uterine section is not different from that of the wild-type (E) except for a smaller diameter. The *inset* in each of these panels shows the glandular apparatus indicating normal estrogenic action in wild-type (B) and heterozygous animal (E). In marked contrast, these estrogenic actions are sparse in FORKO luminal epithelium characterized by a less complex glandular apparatus (H, inset). Cross sections of vaginal tissue (C, F, and I) are at magnification, 50×. The wild-type vaginal section shows a normal stroma (st) and hypertrophied epithelium (ep) (C). In contrast, the FORKO vaginal section is characterized by very thin epithelium consisting of 2–3 layers of cells (I). Vaginal smears shown are taken from wild-type (J) and FORKO (K) mice. The vaginal smear from FORKO mouse (K) does not contain estrogen-induced epithelial cornified cells (ep) found in smears from wild-type females (J). Immunohistochemistry (L, M) with antibodies against lactoferrin show that this marker of estrogen action is lacking in FORKO uterine epithelium (M), whereas the protein is expressed at a high level in the wild-type uterine epithelium (L) (100×). Panels N–O illustrate the longitudinal femoral sections of FORKO and wild-type mice stained with hematoxylin and eosin and shown at high magnification (200×). Note the trabecular bone (*asterisk*) in wild-type femoral section is connected and longer (N), whereas the trabecular bone in FORKO females is sparse (O).

Disruption of estrous cycle (Table 2)

Wild-type mice exhibited regular 4 day cycles. Heterozygous mice had prolonged cycles due to extended diestrus and irregular estrus patterns that was not different in terms of vaginal cytology from wild-type females. All wild-type as well as heterozygous females showed signs of estrogen stimulation (full vaginal cornification) during estrus (Fig. 1J). In over 1 yr of observation, none of FORKO females showed evidence of cyclic behavior. Most smears from FORKO mice were composed of leukocytes and occasional epithelial cells (Fig. 1K). Vaginal opening occurred at proestrus in both wild-type and heterozygous mice, but it was never noticed in FORKO mice. In addition, at the age of 6–7 months, all FORKO mice exhibit clitorimegaly (enlargement of the clitoris) compared with wild-type females of same age, a finding that has also been observed in the aromatase knockout females (26).

Sex accessories undergo atrophy

As important players in reproductive phenomena, the uterus and vagina show cyclic and well characterized periodicity in cellular changes and secretions. The very first clue of a major lack of sustaining endocrine influences for the activity of these tissues was their atrophic status as indicated by the weights at the time the mice were killed. The ovarian weight in null mutants was reduced by 58% compared with wild-type littermates (Fig. 2). Histological analysis of ovaries revealed the crucial differences between FORKO and wild-type female mice. The FORKO ovary displayed only primordial and preantral follicles with hyperplasia of interstitial tissue in the middle of the ovary and no functional corpora lutea (Fig. 1G and *inset*). The ovaries from wild-type mice contained different types of follicles from primordial to preovulatory as well as corpora lutea (Fig. 1A). Heterozygous female ovaries showed normal architecture with follicles at different stages of development including corpora lutea (Fig. 1D).

The uterine and vaginal weights in null mutants were reduced by 70% and 40%, respectively (Fig. 2). The thread like uteri from FORKO females was covered with unusual high amount of fat. The uterine histology of FORKO mice showed distinguishing features of the uterus deprived of estrogen with severely reduced epithelium, stromal, and myometrial layers (Fig. 1H). The glandular elements of the endometrium were less complex in female mutants (Fig. 1H, *inset*) compared with that in wild-type and heterozygous mice (Figs. 1B and 1E, *insets*). The myometrial hypoplasia was more severe in the outer layer of smooth muscle than in the inner layer. The uterine histology of wild-type animals revealed thick myometrial and stromal layers, increased number of the endometrial glands, and multiple epithelial layers in luminal epithelial cells (Fig. 1B). Heterozygous mice at this age showed histology similar to wild-type littermates (Fig. 1E).

Severe vaginal atrophy was also found in all FORKO mice. The vaginal epithelium composed of only 1–3 layers of atrophic epithelial cells (Fig. 1I) showed the absence of cornified epithelial cells in the smear (Fig. 1K). In contrast, vagina from wild-type and heterozygous female mice showed multiple (10–12) stratified epithelial layers (Fig. 1, C and F).

Ovarian steroid hormones

As gross morphological and histological studies showed drastic changes in both these target tissues (Figs. 1 and 2), we suspected an imbalance or a complete absence of estrogen and progesterone, two of the most critical and major ovarian steroid hormones in the female. Steroid measurements by sensitive RIAs revealed virtually complete reduction ($>95\%$) of circulating estrogen in all FORKO females of 3–4 months age (Fig. 3A). Interestingly, the plasma level of estradiol in heterozygous females also showed a decreasing trend (8.2 ± 4.02 pg/ml) compared with wild-type animals (14.2 ± 1.9 pg/ml), but this was not significant due to variations among animals. Progesterone in mutants was also reduced by 70%, compared with the wild-type controls (0.8 *vs.* 2.8 ng/ml) (Fig. 3B). The 30% reduction in serum progesterone for the heterozygous females was also significant. These observations are consistent with the lack of mature follicles in null mutants.

As testosterone is the precursor for estrogen synthesis, we also measured this hormone in circulation. In stark contrast to the estrogen and progesterone levels, testosterone was increased about 10-fold in FORKO mice compared with wild-type animals (Fig. 3C). Heterozygous mice also had slightly elevated level of testosterone. When FORKO mice were ovariectomized, testosterone disappeared from circulation within 4 days (data not shown).

Because the conversion of androgen to the phenolic steroid estrogen is under the influence of aromatase, an enzyme of the cytochrome P450 gene family (26, 27), and FSH action is known to stimulate the enzyme activity (28), we assessed the expression of the gene and protein in all mice. Surprisingly, RT-PCR using specific primers revealed no differences in aromatase expression in the ovary of the three genotypes (Fig. 4A). The predicted 504-bp fragment was correctly amplified in all ovarian samples. There was no expression of the aromatase gene in the uterus, indicating specificity of the amplification reaction. Simultaneous examination of the cyclophilin message in each test sample including the uterus confirmed equivalent amplifications. Western blot analysis of ovarian extracts also did not reveal any difference, and the correct size protein band (54 kDa) was detected in all (Fig. 4B). These observations were highly reproducible.

Body weight and obesity

At 3–4 months of age, it became evident that the mutant females housed and fed under identical conditions were larger and heavier. A comparison of their body weights revealed a definite tendency toward obesity in proportion to disruption of the FSH-R gene. The body weights of the FORKO and heterozygous animals were consistently 20% and 9.6% higher (Fig. 5A). Interestingly, it is known that similar effects are also seen after ovariectomy of normal FSH-R intact mice (29). Virtually all FORKO females revealed an increased deposition of abdominal fat (Fig. 5C). As noted above (Fig. 1), the thin uterus lies buried under copious amount of fat. The total weight of adipose tissue including

abdominal, inguinal, and retroperitoneal fat pads was increased about 2-fold in FORKO mice (Fig. 5B) (600 mg *vs.* 335 mg). Although the body weight of 3–4 month-old heterozygotes does not differ significantly from the wild-type littermates, around 10–12 months of age, all heterozygous females become obese (data not shown). This age-dependent phenomenon in heterozygous mice may be related to the accelerated loss of reproductive function induced by partial FSH-R gene disruption. In marked contrast to the condition of mutant females, obesity was not evident in the homozygous FORKO males at any age (unpublished data), even though all these mice show reduced levels of testosterone.

Skeletal abnormalities in mutant females

Beginning around 4–5 months of age, we began to notice the appearance of a hump in the back of mutants, suggesting a sharp change in the curvature (bending) of the spinal column. All mutants showed the hunchback appearance and could not be laid flat due to the pivoting back unless secured to the dissecting board. Such a stooped posture-kyphosis (also called dowager's hump) is reminiscent of a similar phenomenon in many postmenopausal women as they age and experience loss of estrogen. Because these changes were not apparent in the wild-type, we continued the observation until about a year. Simple x-ray examination of the skeleton revealed the obvious hump in the upper thoracic vertebrae of 4-month-old FORKO female mice (Fig. 6A). At 4 months of age, the skeleton of wild-type mice showed a smooth curve

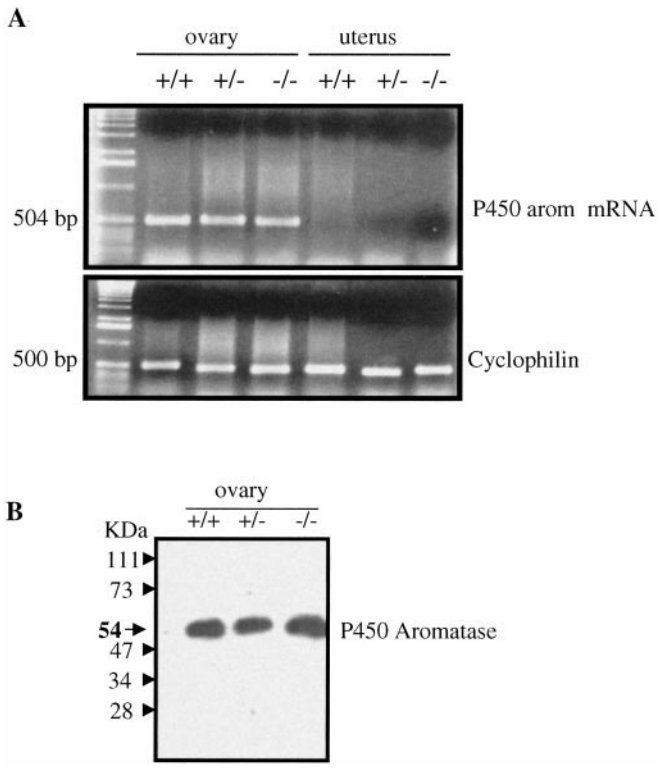

FIG. 4. Ovarian and uterine expression of aromatase. Gene expression was examined at the mRNA and protein levels in tissues from +/+ (wild-type), +/− (heterozygous), and −/− (FORKO) littermates at 3 months of age. A, RT-PCR analysis. Total RNA was extracted and subjected to RT-PCR analysis using primers specific for the mouse sequence as in methods. Correct amplification of the 504-bp target was confirmed by digestion with *Pst*I and *Bam*HI digestions. Cyclophilin amplification is shown as control in each RT-PCR. B, Protein extracts (50 μg) of the ovaries of 3- to 3.5-month-old +/+, +/−, and −/− mice were subjected to Western blotting using antibody to P450 aromatase enzyme. The single 54-kDa signal is seen in all the three lanes.

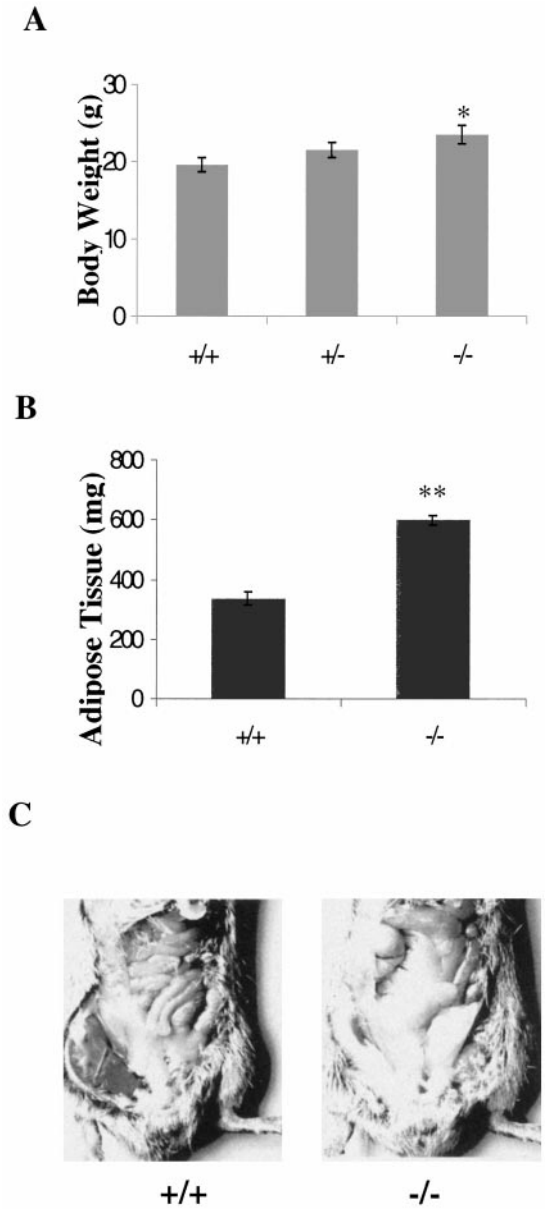

FIG. 5. Evidence of obesity in FORKO mice. A, Body weights (g) of 3- to 3.5-month-old +/+ (wild-type), +/− (heterozygous), and −/− (FORKO) female littermates are shown. The difference of 20% between +/+ and −/− animals is statistically significant (*, $P < 0.05$). The heterozygotes also increased by 9.6% compared with +/+. B, The abdominal adipose tissue collected from each animal was weighed to the nearest mg. Values are expressed as the mean ± SEM. The increase in adipose tissue (162%) was also highly significant (**, $P < 0.004$) when normalized to a 100 g body weight (data not shown). C, The dissected abdominal areas of 3-month-old wild-type (+/+) and FORKO (−/−) littermate females are shown. Note the excessive amount of fat along with increase in the size of the abdomen in FORKO (−/−) mouse.

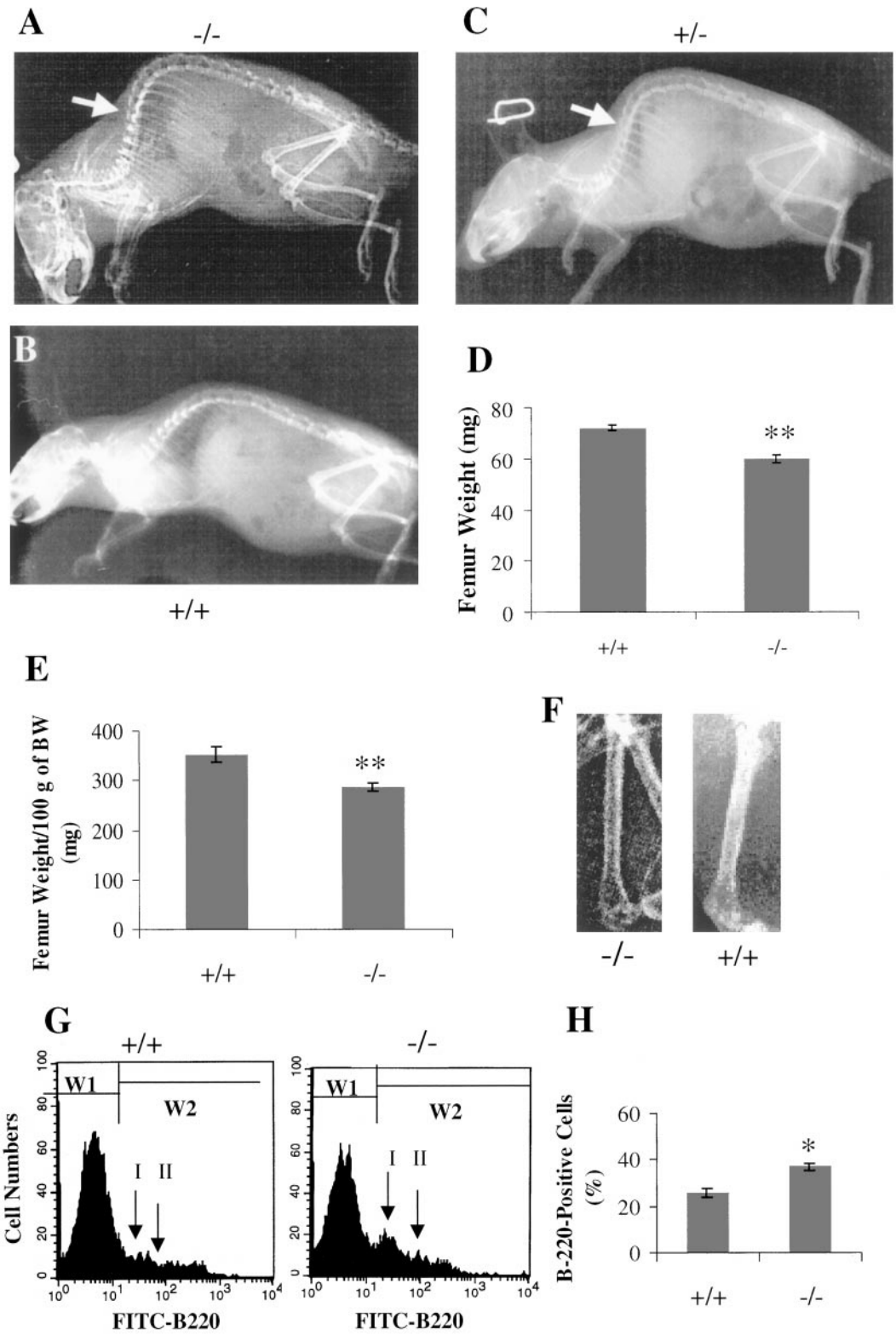

FIG. 6. Skeletal changes in FORKO mice. A, Following anesthesia, x-ray of the whole body was taken with animal placed on its lateral right side. The *arrow* indicates the obvious hump in the thoracic vertebrae in the 4-month-old FORKO female. Due to curvature of the spinal column near the shoulders the thoracic region in these null mutants were protruding prominently. B, X-ray scan of the normal female mouse at 5 months. C, The x-ray scan of the heterozygous mouse at 1 yr is shown to highlight severity that occurs during aging in a condition of sustained estrogen deficiency. D, The weight of right femur was measured in 3- to 3.5-month-old wild-type (wild-type) and −/− (FORKO) littermates. The femora were cleaned of surrounding muscle tissue and weighed to the nearest mg. In this experiment, all the measurements were made blindly without knowing the genotype. Values represent the mean ± SEM for 10 animals per each genotype (**, $P < 0.0005$). E, Femur weight per 100 g of body

(Fig. 6B), and none of the abnormalities noted above were apparent up to 16–18 months in these animals (data not shown). In mutants, this deformity became more acute with aging, and we estimate that at 1 yr there may be as much as 10% vertebral compression accounting for the severe change in posture (data not shown). Interestingly the heterozygous female mice, that show early reproductive senescence, also exhibit skeletal abnormalities characterized by quite a severe deformity at about 1 yr. (Fig. 6C). The absolute weight of femur (61 *vs.* 71 mg) (Fig. 6D) or the weight of this bone per 100 g of body weight in FORKO animals compared with wild-type females (287 *vs.* 352 mg) (Fig. 6E) was significantly reduced. The 16–20% reductions noted for a single bone may be suggestive of the overall fragility and probable osteopenia of the skeletal system in the mutants. In addition, x-ray revealed marked bone loss in the distal methaphysis of the cancellous bone of the femur in FORKO mice, as compared with wild-type (Fig. 6F). The reduced radiopacity in the FORKO mice was observed mainly in the epiphyseal and metaphyseal bone areas. Histological analysis of femoral sections further confirmed the significant loss of trabecular bone in the FORKO mice, compared with wild-type littermates (see color photo in panels O and N of Fig. 1).

Estrogen deficiency caused by ovariectomy has been reported to cause selective stimulation of B-lymphopoiesis (30) resulting in accumulation of pre-B cells in the bone marrow of animals. As this has also been linked to formation of bone resorbing cytokines (31) that function via their specific receptors, we have analyzed pre B-lymphocytes using known markers. The data shown in Fig. 6G reveal that at about 4 months of age, when external signs of skeletal abnormality had already become evident in the mutants, there is an increase in the percentage of pre B-lymphocytes among the cells flushed from the bone marrow. These distinct populations detected by using the specific B-220 antibody are clearly separable by flow cytometric analysis. In the wild-type animal, B220-positive cells were separated into two subpopulations, peak I (B220 ^{low}) and peak II (B220 ^{high}) (Fig. 6G). In FORKO mice, there was a shift as most of the B220-positive cells appeared in peak I, although peak II was also present (Fig. 6G). By setting appropriate windows (W2 in Fig. 6G) during flow cytometric analysis, we estimated the percentage of cells. The proportion of B220-positive cells was markedly increased in FORKO mice compared with the wild-type controls (37% *vs.* 28%) (Fig. 6G).

The nuclear receptor system in target organs

Estrogen action is mediated by at least two nuclear receptors ERα and ERβ (21, 22), which have been characterized in several species including the mouse (32, 33). In view of the induction of estrogen insufficiency from the prepubertal period (Fig. 3A), the question arose whether the estrogen receptor system including signaling functions remain intact in the responsive tissues. To study the relative abundance and the changes of both ER α and ER β mRNA in the uteri and ovaries of mice, we first compared the status of gene expression by RT-PCR (Fig. 7A). For both these genes, the predicted fragments of 411 bp and 203 bp were correctly amplified. There were no differences in the ovarian expression of ER α and β mRNA among all three genotypes in either the uterus or the ovary. The relative abundance of the genes for *e.g.* of the ER α in the uterus and ER β in the ovary in the mouse is generally in accordance with other reports (33, 34). The amplification of cyclophilin gene used as a control validates the comparisons. These gene expression data are further corroborated by the immunological detection of the corresponding protein(s) of the expected size in Western blots, performed by using respective antibodies (Fig. 7B). For the ER α the two monoclonal antibodies gave identical results identifying the correct size 66-kDa band. However, this was not the case with the polyclonal antipeptide ER β antibody that was available for our investigation. Although this antiserum detected a single 54-kDa protein in mouse uterine samples (see Fig. 7B), additional high molecular mass bands were seen in ovarian blots under identical conditions of the experiment. Notwithstanding this difference between the two tissues, it is clear that the intensity of the fainter 54-kDa band as the presumptive ER β remained the same in all the ovarian samples.

Target genes under estrogenic control

As the actions of estrogen on the uterus induce many genes such as lactoferrin, an iron-binding glycoprotein (35), and progesterone receptor (PR) (36), we investigated these proteins in FORKO uterus. A low level of constitutive lactoferrin expression was evident in FORKO uterus (color photo Fig. 1M). In contrast, wild-type females expressed abundant lactoferrin, and the cytoplasmic staining was predominantly confined to the luminal and glandular epithelium (Fig. 1L). The observed luminal staining in the uterus of wild-type corresponds to the presence of secreted lactoferrin, indicating a well-stimulated state. In the FORKO mouse uterus, the PR (which occurs in two forms called A and B) produced from the usage of two promoters (37, 38), appears to be altered compared with the wild-type (Fig. 8, *top*). The PR monoclonal antibody identified the two corresponding bands of 116 kDa and 82 kDa. Interestingly, although both PR-A and B were altered in the heterozygous and FORKO mice, the reduction appeared to be greater in the latter. When we quantitated the bands by densitometry (Fig. 8, *bottom*), a

weight was calculated and also found to be highly significant (**, $P < 0.0005$). F, X-ray was also taken with mice secured in a position on its back with external rotation of lower extremities and fixation with scotch tape. The images of right femora were enlarged identically for all the animals. Note that marked bone loss occurred in the distal metaphysis of the femoral cancellous bone in the FORKO mice compared with the wild-type controls. G, Flow cytometric analysis. Bone marrow cells flushed from the tibia of 3- to 3.5-month-old +/+ (wild-type, n = 4) and −/− (FORKO, n = 4) animals were stained with fluorescein isothiocyanate (FITC)-conjugated B220 antibody specific for lymhopoietic cells. The number of B220-positive cells in bone marrow was counted by flow cytometric analysis. B220-positive cells from +/+ (wild-type) mice were classified into two subpopulations, peak I (B220^{low}) and peak II (B220^{high}). H, The cells in window M2 in panel E for each genotype were quantitated. The percentage of B220-positive cells was significantly increased in the FORKO mice compared with wild-type (37% *vs.* 26%, respectively). Values represent the mean ± SEM for four animals per group. *, $P < 0.05$. For color pictures of bone histology, please see Fig. 1, panels N and O.

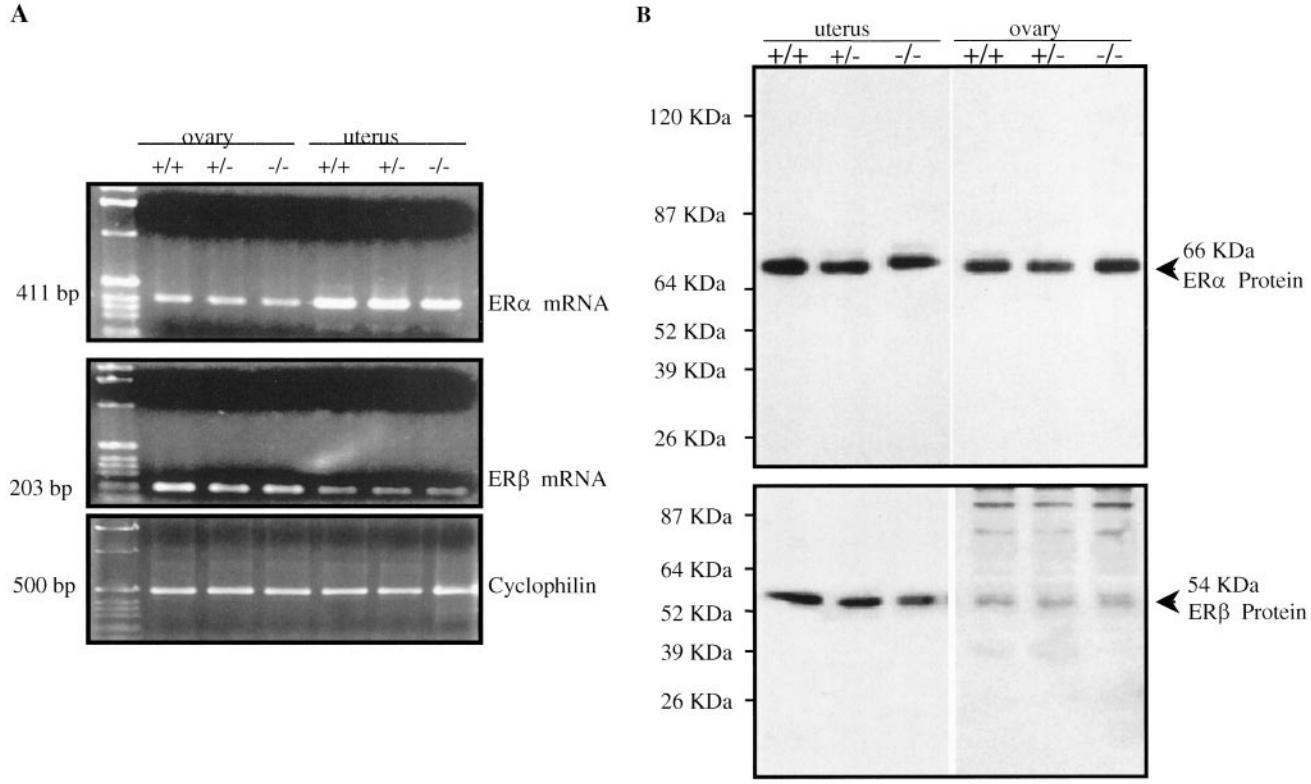

FIG. 7. Ovarian and uterine expression of ERα, ERβ genes, and protein. The expression of these genes was examined at the mRNA and protein levels in tissues from +/+ (wild-type), +/− (heterozygous), and −/− (FORKO) littermates at 3 months of age. A, RT-PCR analyses of ERα (411 bp) and ERβ (203 bp) in the ovary and uterus using primers specific for the mouse sequence as indicated in methods. Cyclophilin amplification is shown as control in each RT-PCR. All PCRs were conducted under identical conditions and are therefore comparable. B, Protein analysis of estrogen receptors. Total proteins were extracted from the ovaries and uteri of 3- to 3.5-month-old +/+, +/−, and −/− mice and were subjected to Western blot analysis using respective anti-IgG (monoclonal for ERα and polyclonal for ERβ).

slightly differential impact was apparent. In the heterozygous uterus, PR-A (-64%) was reduced more than PR-B (-44%) compared with the wild-type controls. In the FORKO uterus, each form of PR was down by 60%.

Estrogen effects on selected targets in FORKO mice

We instituted short-term hormone replacement therapy to verify if estrogen actions are intact. Uterine response was evident in all FORKO mice 48 h after estradiol-17β injection. In addition to water imbibitions (data not shown), uterine weight also increased 2.2-fold over the oil-treated FORKO controls (Fig. 9A). As expected, the uterine weight also increased in estradiol treated wild-type mice. Typical signs of full estrogen stimulation became apparent upon histological examination of the uteri of treated FORKO mice (Fig. 9, B and C). Both stroma and depth of the glandular epithelium increased. As an example of a slightly longer treatment, we administered estrogen for two weeks to evaluate effects on the adipose tissue (see Fig. 5D). This treatment decreased fat mass in FORKO and wild-type females. The decrease in FORKO mice (66%) was greater than in wild-type mice (48%).

Discussion

The targeted disruption strategy that we have used to eliminate the expression of all forms of the FSH-R (4) has resulted in a novel genetic model called the FORKO mouse. This model might be useful in better understanding the physiological implications of FSH-R signaling and investigating the actions of estrogenic hormones in a deficient environment. Complete lack of FSH-R signaling produces interruption of ovarian cycles, infertility, estrogen deprivation, and structural alterations of the uterus and vagina in female mice that arise as a direct consequence of ovarian failure. These results offer experimental evidence for the critical role of FSH-R signaling in the final phases of ovarian follicular development and maturation.

The growth patterns of the ovarian follicles compared by histological and functional analysis for all the genotypes pinpoint that, in absence of the FSH-R signaling, these structures fail to progress beyond the secondary stage and that no other mechanism is able to compensate for this loss. Consequently they become dysfunctional, probably due to increased apoptosis (39). The slight reduction in cyclin D2 gene we observed earlier (4) might also be accompanied by an alteration in protein levels to compromise the proliferation of granulosa cells. In some of the largest follicles in the mutants, no more than four layers of granulosa cells could be seen (Fig. 1G). Thus, cyclin D2 is a possible downstream regulator for maturation. These data are in accord with the report that cyclin D2 null females are infertile even though they retain FSH response (40).

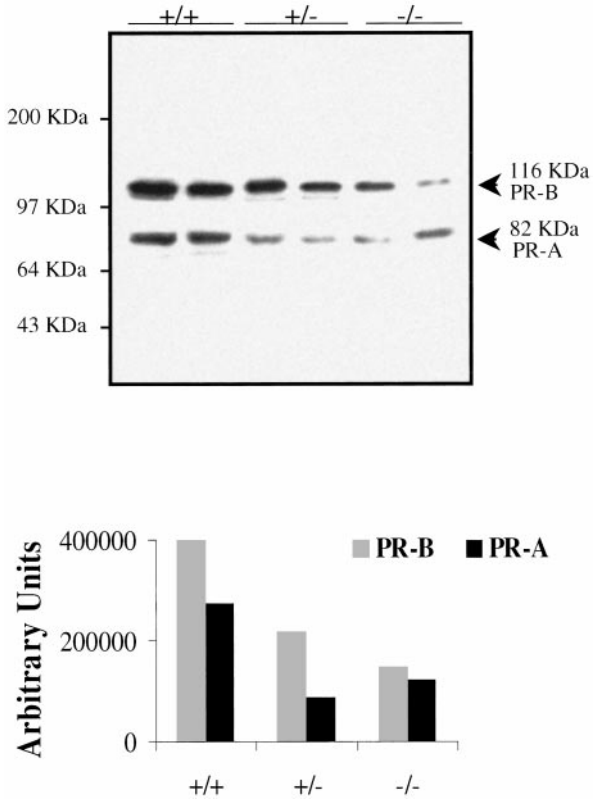

FIG. 8. Progesterone receptor status in the uterus. *Top,* Uterine extracts were prepared and analyzed as in Fig. 7B except that PR monoclonal antibody was used. Shown in this panel are the detection of PR-A and PR-B forms of the progesterone receptor using a monoclonal antibody that recognizes both receptors. At the *bottom panel*, differences in PR that are apparent in the mutants were quantitated by densitometry and shown as arbitrary units.

Sterility in the null FORKO females is clearly due to acyclicity and failure of ovulation. The lack of any of sign recovery of ovarian activity despite the 10-fold rise in hormone (FSH) concentration in serum (4) clearly indicates the absence of any other signaling pathway that could have compensated the lack of FSH-R. The developmental and reproductive senescence of the heterozygous females may also be of potential interest in understanding the incidence of infertility in middle-aged women. The consistent reduction in fertility of the heterozygous mice signifies that the partial failure of the FSH-R signaling system must have had cumulative age-related consequences. This can be inferred by the fact that the heterozygous females that were initially fertile, albeit at a reduced rate, underwent early reproductive senescence. This suggests premature exhaustion of ovarian reserves at an early stage (7–9 months), a time when the wild-type females continue to breed successfully with the same male partners. These observations also suggest that induction of premature ovarian failure may be associated with the loss of a single FSH-R allele. While the exact cellular and molecular basis of this accelerated reproductive senescence remains to be established, we are tempted to propose enhanced apoptosis (39) as a working hypothesis. This process, along with a continual decline in the capacity of the follicles to produce estrogen, may render both the ovary and the uterus com-

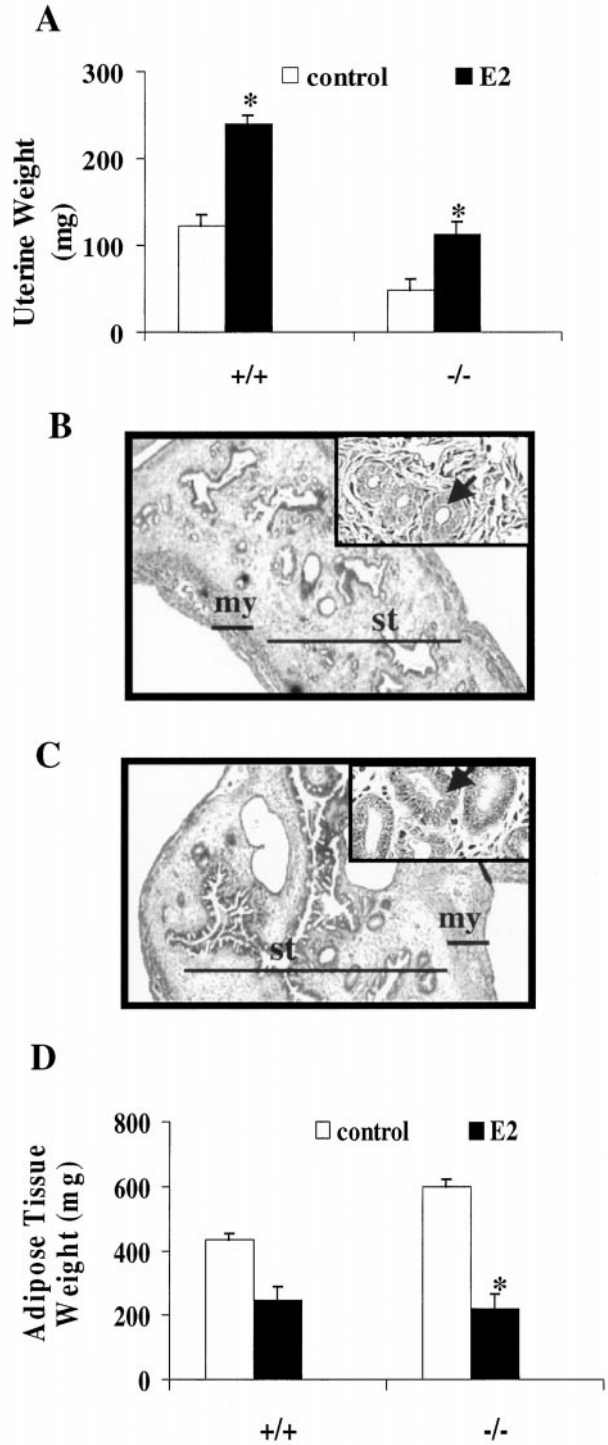

FIG. 9. Effects of estrogen replacement therapy in FORKO females. A, Uterine weights of mice treated with estradiol-17β for 48 h are compared. Control animals received olive oil, and experimental mice received 1 μg estrogen/day for 2 days. *, Statistically significant difference from controls. B and C show histology of the FORKO mouse uterus before and after estrogen treatment. Note growth and hypertrophy of the stroma (st) and glandular epithelium (*inset*) in C. my, Myometrium. Magnification is 12.5 for B and C and for *inset* 200× (D). Similar treatment of FORKO females except that daily treatment (1 μg per day) was extended for 2 weeks. Adipose tissue was collected and weighed. There was a 66% reduction in FORKO mice.

pletely dysfunctional. The apoptosis hypothesis is consistent with corollary observations reporting the extension of functional life of the ovary beyond its normal genetic set point when an apoptotic gene like Bax is inactivated (41).

The infantile nature of the uterus and vagina is fully consistent with the lack of estrogen in the circulation of the mutants. The mammary gland, which is also an estrogen-dependent target tissue was almost unrecognizable in these mutants and consequently no histology of this tissue could be performed in our mice. The absence of estrogen secretion in FORKO females is in sharp contrast to the hormone (FSH β) knockout mouse, where serum estrogen levels are reported to be completely normal (19). Because these FSH β mutants have an elevated level of structurally similar hormone lutropin and an intact FSH-R system in the ovary, the possibility of some cross signaling by this or other mechanisms to sustain adequate levels of estrogen remains a distinct possibility. However, these null females are also sterile, perhaps for different reasons.

With respect to estrogen deficiency, the recently reported ARKO (aromatase knockout) mice are similar in some respects to the FORKO females. The former mutants (26, 42) lack functional aromatase enzyme that can convert testosterone to estradiol-17 β. Interestingly, in both types of these mutants, there is an accumulation of testosterone in the circulation (Fig. 3C). The ovarian origin of high androgen in our mutants was proven because it promptly disappeared from circulation after bilateral ovariectomy. Our findings of a normal pattern of the aromatase gene and protein expression (Fig. 4, A and B) in the FORKO mutants are intriguing. This shows that while the expression of the aromatase gene and its product in the granulosa cells of the ovary is not dependent on FSH-R signaling, activation of the preexisting enzyme may be involved to allow conversion of androgen into estrogen, once the hormone receptor is activated. In the absence of such an activation mechanism, the substrate testosterone accumulates in circulation (Fig. 3C). Thus, it appears that in the FORKO mouse no other mechanism is able to substitute for activating the ovarian aromatase enzyme in the complete absence of the FSH-R signaling.

Based on the evidence from this study, the FORKO mouse becomes an experimental animal model imitating many of the symptoms of menopause in women. The lack of estrogen in FORKO females produced three major and recognizable phenotypes—infertility, obesity, and skeletal abnormality, all of which became apparent and visible externally within a few months. The persistence of all these changes with 100% penetrance is an indication of the critical role of ovarian estrogen in these functions. Only some of these phenotypes have been reported in other related knockout models like the ARKO (26), BERKO (32), ERKO (21), the FSH β (19), cyclin D2 (40), to name a few that have been recently reported to develop ovarian dysfunction of different types. Because of the expression of two separate receptor genes, deletion of one of the ERs might permit residual activation or up-regulation of the other nuclear receptor-signaling pathways, producing compensation in tissues that may express both receptors (33). In the FORKO females, production of the ligand (estradiol 17-β) itself is severely curtailed to undetectable levels. While the generation of some related estrogenic compound that did not react in the immunoassay cannot be ruled out, such a compound if produced fails to interact with the estrogen receptors because sex accessories remain atrophied. We note that the accelerated ovarian senescence in the heterozygous mice duplicates the cessation of cycles in middle aged women. Because both the brain and ovary are major pacemakers of aging and menopause (43), further studies on FORKO mice might be helpful in defining the candidate genes that are involved.

The three phenotypes that we have characterized at present in FORKO females substantiate some of these clinical and epidemiological observations on menopause to suggest the use of these mice as a model in understanding the ramifications of hormone replacement therapy. This becomes feasible only if one or both (or all) ER genes are intact and signaling aspects remain fully functional. The data we have shown in Fig. 7 for these genes in selected tissues are confirmed by the examples of prompt estrogen response at two disparate sites (see Fig. 9), suggesting that preservation of the same system(s) at other targets is highly probable. Differentiating and dissociating the beneficial effects of estrogens such as protection of the cardiovascular system and prevention of osteoporosis from its undesirable proliferative stimulus on the breast and uterus is a challenging task. This has led to significant progress in the development of Selective Estrogen Receptor Modulators (SERMs) (44). We suggest that the FORKO mice may be suitable in evaluating their potential benefits because the ER signaling pathways remain unaffected. The changes that appear in heterozygous females are also interesting and significant for two important reasons. First, according to our knowledge, no other gene disruption in the reproductive system has been shown to develop such a strong partial phenotype in the heterozygotes that intensifies in the homozygous genotype. Second, the same external phenotypes like obesity and kyphosis that are evident in the null mutants at an early age manifest themselves later in the heterozygotes. The reduced fertility in heterozygous females is probably due to inappropriate steroid secretion as well as an imbalance in the progesterone receptor that may create a hostile environment in the uterus not conducive for maintaining full fertility.

The distribution of fat mass in the abdomen (Fig. 5) of FORKO mice parallels the situation in postmenopausal women, many of whom also gain weight. Although the intricate effects of numerous regulatory interactions that influenced fat deposition are unknown, it is clear that young FORKO mice show the obese tendency. It is interesting that estrogen replacement eliminated the excess adipose tissue mass in FORKO mice, indicating its metabolic effects (Fig. 9). That this normalizing effect occurred in a background of high testosterone in FORKO mice indicates that it was of no consequence to derive the benefits of estrogen replacement.

Estrogen loss in women causes osteoporosis and ovariectomy in the rat induces rapid osteopenia and elevated bone turnover (45, 46). Osteoporosis changes the curvature of the spine, inducing kyphosis in the upper thoracic vertebrae in postmenopausal women. The appearance of similar effects in

FORKO mice may be directly attributable to estrogen loss. Our flow cytometric detection of higher proportion of B-220-positive cells in FORKOs agree well with several other findings of the role of sex steroids in the regulation of B-lymphopoiesis (25, 30). Whether the apparent high level of testosterone in the FORKO mutants might cause some of the changes we have observed cannot be answered at this time. At any rate, it is clear that the high androgen level is unable to substitute for the lost effects of estrogen on the bone and other tissues. This also indicates that any peripheral conversion of androgen to estrogen in the null mutants is unlikely to be of practical significance. We see similar skeletal changes in aging FORKO males (unpublished data), indicating that declining androgen levels may contribute to osteoporosis.

In conclusion, we have shown the dysfunction in ovarian steroidogenesis, cyclicity, and urogenital morphology along with obesity and skeletal abnormalities in FORKO female mice. This gene knockout offers a unique and potentially useful animal model for advancing our knowledge on the physiology and molecular mechanisms of gonadal receptors and hormones.

Acknowledgments

The assistance of Mr. Rouslan Kats in maintaining the mice and genotyping are greatly appreciated. We also thank Drs. P. Chambon, G. L. Greene, C. Teng, E. R. Simpson, and P. T. K. Saunders for the kind gift of antibody reagents used in the study. The staff members of the bone unit at the Shriners Hospital for Children in Montreal are thanked for their assistance in x-ray of mice. The editorial assistance of Odile Royer is greatly appreciated.

References

1. **Pierce JG, Parsons TF** 1981 Glycoprotein hormones: structure and function. Annu Rev Biochem 50:465–496
2. **Sairam MR** 1999 Gonadotropins: overview. In: Knobil E, Niell JD (eds) Encyclopedia of Reproduction. Academic Press Inc., New York, pp 552–565
3. **McFarland KC, Sprengel R, Phillips HS, Kohler M, Rosemblit N, Nikolics K, Segaloff DL, Seeburg PH** 1989 Lutropin-choriogonadotropin receptor: an unusual member of the G protein-coupled receptor family. Science 245: 494–499
4. **Dierich A, Sairam MR, Monaco L, Fimia GM, Gansmuller A, LeMeur M, Sassone-Corsi P** 1998 Impairing follicle-stimulating hormone (FSH) signaling *in vivo*. Targeted disruption of the FSH receptor leads to aberrant gametogenesis and hormonal imbalance. Proc Natl Acad Sci USA 95:13612–13617
5. **Sprengel R, Braun T, Nikolics K, Segaloff DL, Seeburg PH** 1990 The testicular receptor for follicle stimulating hormone: structure and functional expression of cloned cDNA. Mol Endocrinol 4:525–530
6. **Sairam MR, Jiang LG, Yarney TA, Khan H** 1997 Alternative splicing converts the G-protein coupled follitropin receptor gene into a growth factor type I receptor: Implications for pleiotropic actions of the hormone. Mol Reprod Dev 48:471–479
7. **Heckert LL, Daley IJ, Griswold MD** 1992 Structural organization of the follicle-stimulating hormone receptor gene. Mol Endocrinol 6:70–80
8. **Sairam MR, Subbarayan VSR** 1997 Characterization of the 5′ Flanking region and potential control elements of the ovine follitropin receptor gene. Mol Reprod Dev 48:480–487
9. **Babu PS, Jiang J, Sairam AM, Touyz RM, Sairam MR** 1999 Structural features and expression of an alternatively spliced growth factor type I receptor for follitropin signaling in the developing ovary. Mol Cell Biol Res Commun 2:21–27
10. **Lapthorn AJ, Harris DC, Littlejohn A, Lustbader JW, Canfield RE, Machin KJ, Morgan FJ, Isaacs NW** 1994 Crystal structure of human chorionic gonadotropin. Nature 369:455–461
11. **Robker RL, Richards JS** 1998 Hormonal control of the cell cycle in ovarian cells: proliferation versus differentiation. Biol Reprod 59:476–482
12. **Aittomäki K, Dieguez Lucena JL, Pakarinen P, Sistonen P, Tapanainen J, Gromoll J, Kaskikari R, Sankila EM, Lehväslaiho H, Engel AR, Nieschlag E, Huhtaniemi I, de la Chapelle A** 1995 Mutation in the follicle-stimulating hormone receptor gene causes hereditary hypergonadotropic ovarian failure. Cell 82:959–968
13. **Aittomaki K, Herva R, Stenman UH, Juntunen K, Ylostalo P, Hovatta O, de la Chapelle A** 1996 Clinical feature of primary ovarian failure caused by a point mutation in the follicle stimulating hormone receptor gene. J Clin Endocrinol Metab 81:3722–3726
14. **Tapanainen JS, Aittomaki K, Miu J, Vaskivuo T, Huhtaniemi IT** 1997 Men homozygous for an inactivating mutation of the follicle-stimulating hormone (FSH) receptor gene present variable suppression of spermatogenesis and fertility. Nat Genet 15:205–206
15. **Gromoll J, Simoni M, Nieschlag E** 1996 An activating mutation of the follicle stimulating hormone receptor autonomously sustains spermatogenesis in a hypophysectomized man. J Clin Endocrinol Metab 81:1367–1370
16. **Matthews CH, Borgato S, Beck-Peccoz P, Adams H, Tone Y, Gambino G, Casagrande S, Tedeschini G, Benedetti A, Chatterjee VKK** 1993 Primary amenorrhoea and infertility due to a mutation in the β subunit of follicle-stimulating hormone. Nat Genet 5:83–86
17. **Layman LC, Lee EJ, Peak DB, Namnoum AB, Vu KV, van Lingen BL, Gray MR, McDonough PG, Reindollar RH, Jameson JL** 1997 Delayed puberty and hypogonadism caused by mutations in the follicle-stimulating hormone β-subunit gene. N Engl J Med 337:607–611
18. **Phillip M, Arbelle JC, Seger Y, Pavnari F** 1998 Male hypogonadism due to a mutation in the gene for the β-subunit of follicle stimulating hormone. N Engl J Med 338:1729–1732
19. **Kumar TR, Wang Y, Lu N, Matzuk MM** 1997 Follicle stimulating hormone is required for ovarian follicle maturation but not male fertility. Nat Genet 15:201–204
20. **Katzenellenbogen BS** 1996 Estrogen receptors: bioactivities and interactions with cell signaling pathways. Biol Reprod 54:287–293
21. **Lubahn DB, Moyer JS, Golding TS, Couse JF, Korach KS, Smithies O** 1993 Alteration of reproductive function but not prenatal sexual development after insertional disruption of the mouse estrogen receptor gene. Proc Natl Acad Sci USA 90:11162–11166
22. **Kuiper GG, Enmark E, Pelto-Huikko M, Nilsson S, Gustafsson JA** 1996 Cloning of a novel estrogen receptor expressed in rat prostate and ovary. Proc Natl Acad Sci USA 93:5925–5930
23. **Danilovich N, Sairam MR, Babu PS, Xing W, Gerdes M** 1999 Estrogen deficiency, obesity and skeletal abnormalities in follitropin (FSH) receptor knockout (FORKO) female mice. 55th Annual Meeting of the American Society for Reproductive Medicine, Toronto. Fertility and Sterility [Suppl 1] 72 (Abstract O-075)
24. **Sairam MR, Danilovich N** 1999 The FORKO mouse as a genetic model for hormone replacement therapy. 55th Annual Meeting of the American Society for Reproductive Medicine, Toronto. Fertility and Sterility [Suppl 1] 72 (Abstract P-290)
25. **Masuzawa T, Miyaura C, Onoe Y, Kusano K, Ohta H, Nozawa S, Suda T** 1994 Estrogen deficiency stimulates B lymphopoiesis in mouse bone marrow. J Clin Invest 94:1090–1097
26. **Fisher CR, Graves KH, Parlow AF, Simpson ER** 1998 Characterization of mice deficient in aromatase (ArKO) because of targeted disruption of the cyp19 gene. Proc Natl Acad Sci USA 95:6965–6970
27. **Terashima M, Toda K, Kawamoto T, Kuribayashi I, Ogawa Y, Maeda T, Shizuta Y** 1991 Isolation of a full-length cDNA encoding mouse aromatase P450. Arch Biochem Biophys 285:231–237
28. **Fitzpatrick SL, Richards JS** 1991 Regulation of cytochrome P450 aromatase messenger ribonucleic acid and activity by steroids and gonadotropins in rat granulosa cells. Endocrinology 129:1452–1462
29. **Ke HZ, Paralkar VM, Grasser WA, Crawford DT, Qi H, Simmons HA, Pirie CM, Chidsey-Frink KL, Owen TA, Smock SL, Chen HK, Jee WS, Cameron KO, Rosati RL, Brown TA, Dasilva-Jardine P, Thompson DD** 1998 Effects of CP-336,156, a new, nonsteroidal estrogen agonist/antagonist, on bone, serum cholesterol, uterus and body composition in rat models. Endocrinology 139:2068–2076
30. **Miyaura C, Onoe Y, Inada M, Maki K, Ikuta K, Ito M, Suda T** 1997 Increased B-lymphopoiesis by interleukin 7 induces bone loss in mice with intact ovarian function: similarity to estrogen deficiency. Proc Natl Acad Sci USA 94:9360–9365
31. **Jilka RL, Mangoc G, Girasole G, Passeri G, Williams DC, Abrams JS, Boyce B, Broxmeyer H, Manalagas SC** 1992 Increased osteoclast development after estrogen loss: mediation by interleukin-6. Science 257:88–91
32. **Krege JH, Hodgin JB, Couse JF, Enmark E, Warner M, Mahler JF, Sar M, Korach KS, Gustafsson JA, Smithies O** 1998 Generation and reproductive phenotypes of mice lacking estrogen receptor β. Proc Natl Acad Sci USA 95:15677–15682
33. **Nilsson S, Kuiper GG, Gustafsson JA** 1998 ER β: a novel estrogen receptor offers the potential for new drug development. Trends Endocrinol Metab 9:387–395
34. **Couse JF, Lindzey J, Grandien K, Gustafsson JA, Korach KS** 1997 Tissue distribution and quantitative analysis of estrogen receptor-α (ERα) and estrogen receptor-β (ERβ) messenger ribonucleic acid in the wild-type and ERα-knockout mouse. Endocrinology 138:4613–4621
35. **Pentecost BJ, Teng CT** 1987 Lactotransferrin is the major estrogen inducible protein of mouse uterine secretions. J Biol Chem 262:10134–10139

36. **Lydon JP, DeMayo FJ, Funk CR, Mani SK, Hughes AR, Montgomery CAJ, Shyamala G, Conneely OM, O'Malley BW** 1995 Mice lacking progesterone receptor exhibit pleiotropic reproductive abnormalities. Genes Dev 9: 2266–2278
37. **Graham JD, Clarke CL** 1997 Physiological action of progesterone in target tissues. Endocr Rev 18:502–519
38. **Schneider W, Ramachandran C, Satyaswaroop PG, Shyamala G** 1991 Murine progesterone receptor exists predominantly as the 83-kilodalton 'A' form. J Steroid Biochem Mol Biol 38:285–291
39. **Tilly JL** 1996 Apoptosis and ovarian function. Rev Reprod 1:162–172
40. **Sicinski P, Donaher JC, Geng Y, Parker SB, Gardner H, Park MY, Robker RL, Richards JS, McGinnis LK, Biggers JD, Eppig JJ, Bronson RT, Elledge SJ, Weinberg RA** 1996 Cyclin D2 is an FSH responsive gene involved in gonadal cell proliferation and oncogenesis. Nature 384:470–474
41. **Perez GI, Robles R, Knudson CM, Flaws JA, Korsmeyer SJ, Tilly JL** 1999 Prolongation of ovarian lifespan into advanced chronological age by Bax-deficiency. Nat Genet 21:200–203
42. **Honda SI, Harada N, Ito S, Takagi Y, Maeda S** 1998 Disruption of sexual behavior in male aromatase-deficient mice lacking exons-1 and 2 of the cyp19 gene. Biochem Biophys Res Commun 252:445–449
43. **Wise PM, Krajnak KM, Kashon ML** 1996 Menopause: the aging of multiple pacemakers. Science 273:67–70
44. **El-Hajj Fuleihan G** 1997 Tissue-specific estrogens—the promise for the future. N Engl J Med 337:1686–1687
45. **Turner RT, Riggs BL, Spelsberg TC** 1994 Skeletal effects of estrogen. Endocr Rev 15:275–300
46. **Lim SK, Won YJ, Lee HC, Huh KB, Park YS** 1999 A PCR analysis of ERα and ERβ mRNA abundance in rats and the effect of ovariectomy. J Bone Miner Res 14:1189–1196